# Coupling Impedances in SIS100

V. Kornilov

February 26, 2015

## 1 Transverse Impedance

### 1.1 Resistive Wall Impedance

There are two regimes for the resistive wall impedance depending on the relation between the skin depth $\delta_{\rm sk} = \sqrt{2/\mu_0\sigma\omega}$ and the pipe wall thickness $d_{\rm pipe}$,

$$\text{thick}-\text{wall}\ \ \delta_{\rm sk} < d_{\rm pipe}\ , \omega > \omega_{\rm sk}\ , \qquad \mathrm{Re}\Big(Z^{\perp}_{\rm rw}\Big) = L\frac{Z_0}{2\pi b^3}\ \delta_0\sqrt{\frac{\omega_0}{\omega}}\ , \tag{1}$$

$$\text{thin}-\text{wall}\ \ \delta_{\rm sk} > d_{\rm pipe}\ , \omega < \omega_{\rm sk}\ , \qquad \mathrm{Re}\Big(Z^{\perp}_{\rm rw}\Big) = L\frac{Z_0}{2\pi b^3}\frac{\delta_0^2}{d_{\rm pipe}}\frac{\omega_0}{\omega}\ , \tag{2}$$

where $\delta_0 = \sqrt{2/\mu_0\sigma\omega_0}$ is the skin depth at the revolution frequency, $Z_0 = \mu_0 c \approx 376.7\,\Omega$ and $b$ is the pipe radius; here for the circular chamber. Both regimes of the resistive wall impedance can be described [3] with

$$Z^{\perp}_{\rm rw} = (1-i)L\frac{Z_0}{2\pi b^3}\ \delta_0\sqrt{\frac{\omega_0}{\omega}}\coth\left\{\frac{\omega\, d_{\rm pipe}}{\beta c}\sqrt{\frac{1}{\gamma^2} - i\frac{\sigma\beta^2}{\epsilon_0\omega}}\right\}\ . \tag{3}$$

In the case of SIS100, the pipe wall thickness in the magnet chambers is $d_{\rm pipe} = 0.3\,\mathrm{mm}$, and the border frequency between the skin effect regimes Eqs. (1, 2) is

$$\omega_{\rm sk} = \frac{2}{\mu_0\sigma d^2_{\rm pipe}}, \tag{4}$$

which corresponds to $f_{\rm sk} = \omega_{\rm sk}/2\pi \approx 2\,\mathrm{MHz}$. The quadrupole and dipole chambers make up 60% of the ring circumference. For the rest we assume drift spaces. Parameters which were assumed for the resistive wall impedance at SIS100 are summarized in Table 1.

The resistive wall impedance of an elliptical pipe can be obtained numerically [4]. The results for different radius ratios are presented in Fig. 1. The ratios of the transverse

| | Horizontal Diameter $2b_x$ | Vertical Diameter $2b_y$ | Wall thickness $d_{\rm pipe}$ | Length |
|---|---|---|---|---|
| Quadrupole Chambers | 133.44 mm | 65.21 mm | 0.3 mm | 282.5 m |
| Dipole Chambers | 120 mm | 60 mm | 0.3 mm | 372.6 m |
| Drift Spaces | 135 mm | 65 mm | 3 mm | 428.48 m |

Table 1: Parameters of the SIS100 elliptic pipes assumed here to estimate the resistive wall impedance. The pipe conductivity is $\sigma = 1.4 \times 10^6\,(\mathrm{Ohm\,m})^{-1}$.

real impedance to that of the round pipe Eqs. (1, 2) are shown for the frequency range of interest. The solid lines show the vertical impedance, while the dashed line correspond to the impedance in the horizontal plane. Using these data, and the parameters from Table 1, we obtain the resulting resistive wall impedance for SIS100 and present it in Fig. 2.

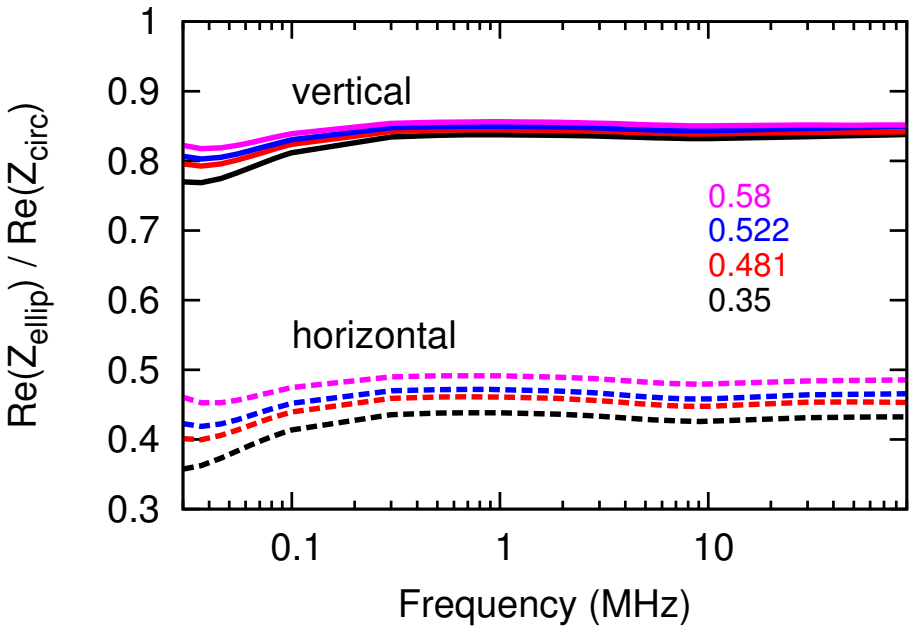


Figure 1: The transverse resistive wall impedance for elliptical pipes. Four axis ratios $b_y/b_x$ are indicated by colors. The results are normalised by the impedance of the circular pipe with $b = b_y$ and $d_{\rm pipe} = 0.3\,\mathrm{mm}$ at the related frequency.

The real part of the transverse resistive wall impedance has a maximum around the

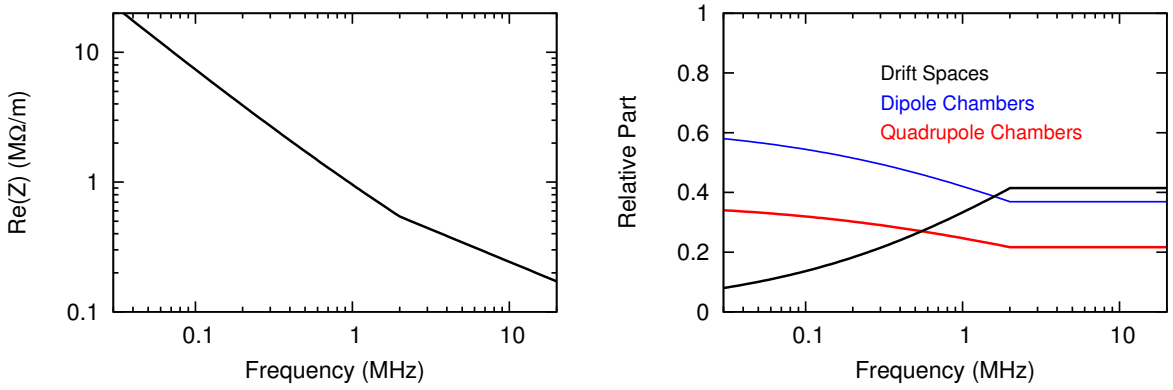


Figure 2: The transverse resistive wall impedance in SIS100. Left-side plot: the total impedance. Right-side plot: relative contributions of the different chamber types, see Table 1.

transition frequency

$$\omega_{\perp \mathrm{bp}} = \frac{2}{b\mu_0\sigma d_{\mathrm{pipe}}}, \tag{5}$$

which is due to the effect of the inductive bypass [2] at low frequencies. For the SIS100 magnet chambers it corresponds to $f_{\perp \mathrm{bp}} \approx$17 kHz. For the collective bunch stability the frequencies above ≈30 kHz are relevant, hence the effects below $f_{\perp \mathrm{bp}}$ are not included in Fig. 2.

## 1.2 Image Charges

The effect of the image charges in a conducting chamber corresponds to an imaginary transverse impedance which shifts the coherent betatron frequency. The coherent tune shift due to image charges can be described by the coefficients $\xi_x, \xi_y, \epsilon_x, \epsilon_y$ for the horizontal $(x)$ and for the vertical $(y)$ plane,

$$\Delta Q_{\mathrm{coh}} = -\frac{\lambda_0 r_p R^2}{\gamma^3 \beta^2 Q_{x,y}} \frac{2\xi_{x,y} + \beta^2\gamma^2 B_{\mathrm{f}} 2\epsilon_{x,y}}{h^2} \ . \tag{6}$$

Here we include the combination of the electric images and the magnetic images in the beam pipe only, the magnetic field is non-penetrating. For the round pipe, $h$ is equal to the pipe radius and $\xi_{x,y} = 0.5, \epsilon_{x,y} = 0$. The line density $\lambda_0$ corresponds to the bunch middle, $r_p = q_{\mathrm{ion}}^2/4\pi\varepsilon_0 m_{\mathrm{ion}} c^2$.

In the case of an elliptical pipe with the horizontal radius $b_x$ and with the vertical radius $b_y$, $b_x > b_y$, the characteristic pipe size in Eq. (6) is $h = b_y$. The coherent shift coefficients can be calculated using [8]

$$\xi_x = \frac{b_y^2}{4(b_x^2 - b_y^2)} \left\{ 1 - \left( \frac{2Kk'}{\pi} \right)^2 \right\} , \tag{7}$$

$$\xi_y = \frac{b_y^2}{4(b_x^2 - b_y^2)} \left\{ \left( \frac{2K}{\pi} \right)^2 - 1 \right\} , \tag{8}$$

$$\epsilon_y = -\epsilon_x = \frac{b_y^2}{12(b_x^2 - b_y^2)} \left\{ (1 + k'^2) \left( \frac{2K}{\pi} \right)^2 - 2 \right\} , \tag{9}$$

where $K(k)$ is the complete elliptic integral of the first kind and $k$ is the modulus, which can be calculated using the complementary modulus $k'$ [8]. The resulting coefficients are presented in Fig. 3. The case $b_y/b_x = 1$ corresponds to the round pipe with $\xi_{x,y} = 0.5, \epsilon_{x,y} = 0$, and for the small radius ratios the coefficients converge to that of the parallel plates, $\xi_x = 0, \xi_y = \pi^2/16, \epsilon_y = \pi^2/48$.

For the SIS100 pipes (Table 1) the coefficients are

| | | | | |
|---|---|---|---|---|
| Quadrupole Chambers | $b_y/b_x = 0.49$ , | $\xi_x = 0.077$ , | $\xi_y = 0.6$ , | $\epsilon_y = 0.17$ |
| Dipole Chambers | $b_y/b_x = 0.5$ , | $\xi_x = 0.082$ , | $\xi_y = 0.6$ , | $\epsilon_y = 0.17$ |
| Drift Spaces | $b_y/b_x = 0.48$ , | $\xi_x = 0.075$ , | $\xi_y = 0.6$ , | $\epsilon_y = 0.18$ |

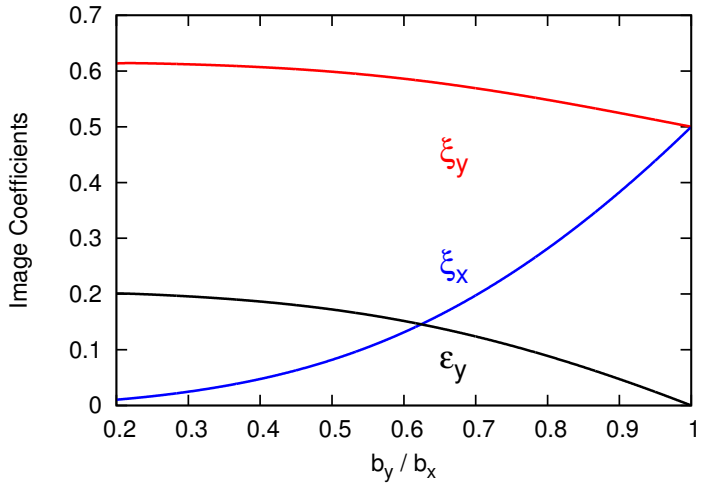


Figure 3: Image charge coefficients for elliptical chambers with different radius ratios, $\epsilon_x = -\epsilon_y$.

The effective transverse impedance of the image charges in a conducting pipe is

$$Z^{\perp} = -i\frac{Z_0 C}{2\pi\gamma^2\beta^2}\frac{2\xi_{x,y} + \beta^2\gamma^2 B_{\mathrm{f}} 2\epsilon_{x,y}}{h^2} \ , \tag{10}$$

where $C = 2\pi R$, $Z_0 = 1/(\varepsilon_0 c) \approx 376.7\,\Omega$. In the case of the vertical plane in SIS100, this impedance corresponds to:

- $Z^{\perp} = -i\,190\,\mathrm{M}\Omega/\mathrm{m}$ for the heavy ion injection energy (0.2 GeV/u);
- $Z^{\perp} = -i\,20\,\mathrm{M}\Omega/\mathrm{m}$ for the heavy ion extraction energy (1.5 GeV/u);
- $Z^{\perp} = -i\,1.8\,\mathrm{M}\Omega/\mathrm{m}$ for the proton extraction energy (29 GeV/u).

## 1.3 Broad-Band Transverse Impedance

The broad-band resonator model is usually used to approximate the complete impedance of the numerous elements of the facility,

$$Z^{\perp}_{\mathrm{bb}} = \frac{\omega_r}{\omega}\frac{R_{\perp}}{1 + iQ_{\mathrm{bb}}\left(\frac{\omega}{\omega_r} - \frac{\omega_r}{\omega}\right)} \ , \tag{11}$$

with the shunt impedance $R_{\perp}$, the quality factor $Q_{\mathrm{bb}} = 1$, and the resonant frequency $\omega_r$. The transverse shunt impedance can be estimated from the longitudinal one,

$$R_{\perp} = \frac{2R}{b^2\beta}\left|\frac{Z_{\parallel}}{n}\right| \ . \tag{12}$$

Using the assumption about the longitudinal broad-band impedance Eq. (20), we obtain $R_{\perp} \approx 7\,\mathrm{M}\Omega/\mathrm{m}$. The resonant frequency corresponds to the cutoff frequency Eq. (15) $f_r \approx 1.5\,\mathrm{GHz}$. The resulting impedance is shown in Fig. 4. In the case of the CERN PS synchrotron, the vertical $R_{\perp} \approx 3\,\mathrm{M}\Omega/\mathrm{m}$ and the horizontal $R_{\perp} \approx 1\,\mathrm{M}\Omega/\mathrm{m}$ have been determined [7].

## 1.4 SIS100 Bipolar Kickers

An important contribution to the SIS100 transverse impedance is expected from the bipolar extraction/emergency kickers. The two circuits of the pulse forming network are visible to the beam and produce large impedances in the vertical plane. Figure 5 presents the results of electronic calculations [4] for the SIS100 kicker, with the usage of the Nassibian-Sacherer model [9],

$$Z^{\perp} = \frac{\beta c\omega\mu_0^2 l^2}{4a^2 Z_k} \ , \tag{13}$$

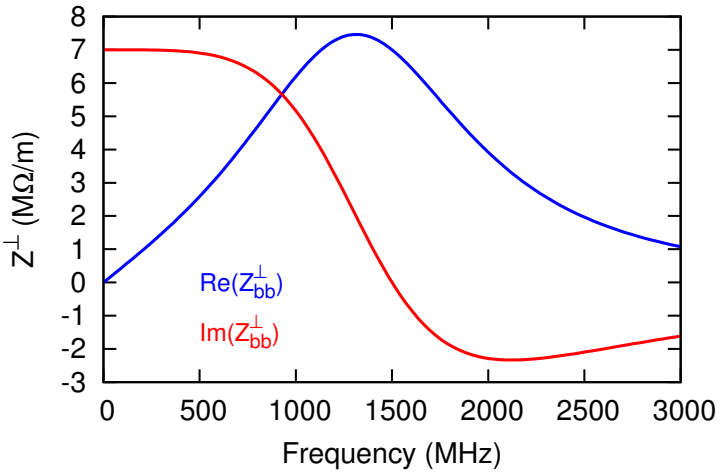


Figure 4: The SIS100 transverse broad-band impedance model.

where $Z_k = i\omega L + Z_g$ is given by the network. The impedance is shown for $\beta = 1$, for one kicker module. Eight modules of the extraction/emergency kickers should be installed in SIS100.

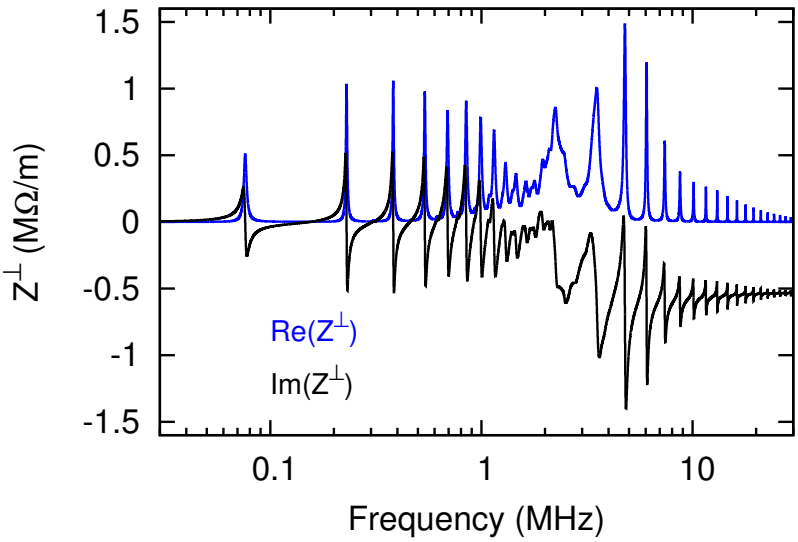


Figure 5: The vertical impedance given by the network of the SIS100 extraction/emergency kicker. Contribution of one module is shown, the impedance scales with the relativistic $\beta$.

The ferrite yoke of the bipolar kicker also has an impedance contribution. Preliminary calculations [4] have indicated a negligible transverse impedance $Z^{\perp} < 10\,\mathrm{k\Omega/m}$ for fre-

quencies below 0.1 GHz. It is then reasonable to assume that the transverse broad-band model includes the high-frequency kicker yoke impedance.

## 1.5 Summary for the Transverse Impedance

Figure 6 shows the most important sources of the transverse real impedance in the vertical plane. The SIS100 bipolar kicker impedance is given for the ion injection energy 200 MeV/u, $\beta = 0.566$, for the eight modules. In the horizontal plane, there is no extraction/emergency kicker, the resistive wall should provide approximately a half of the impedance, see Fig. 1, and the broad-band impedance might be similar to that in the vertical plane. The high-frequency contributions from the ferrite loaded kickers, the rf cavities, bellows and steps, constitute the broad-band impedance model.

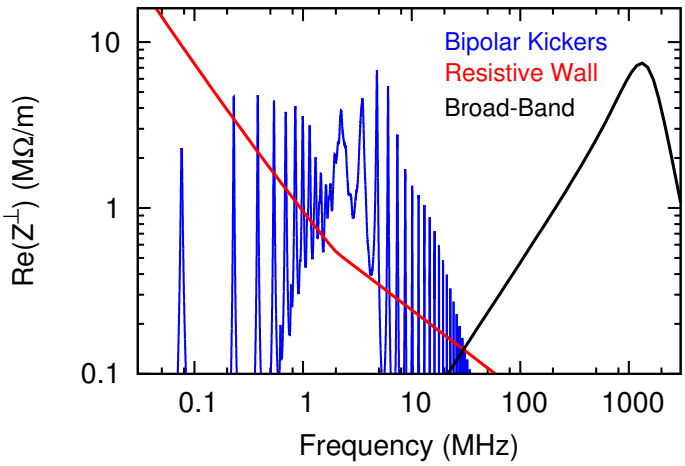


Figure 6: Overview of the main contributions to the real transverse impedance in SIS100.

The imaginary transverse impedance is dominated by the vacuum pipe image charges, especially for the beams at the injection energies, as we discuss above. For the extraction energies, the broad-band impedance and probably also other sources as the resistive wall impedance should be taken into account.

# 2 Longitudinal Impedance

## 2.1 Space Charge

The effect of space charge can be treated as an impedance for the longitudinal plane. For a round uniform distribution beam $a$ in a circular pipe $b$ the corresponding impedance is given by

$$Z_{\rm sc}^{\parallel} = i\frac{\omega}{\omega_0}\frac{Z_0}{\gamma^2\beta}\left(\frac{1}{4} + \ln\frac{b}{a}\right) , \tag{14}$$

below the pipe cutoff frequency

$$\omega_{cut} = \frac{c}{b} , \tag{15}$$

which is $f_{cut} \approx 1.5\,\mathrm{GHz}$ for SIS100.

The absolute value of the space-charge impedance for SIS100 is shown in Fig. 7. The cases of the proton acceleration and the uranium acceleration have different energy ramps, beam parameters. The ramp rate $4\,\mathrm{T/s}$ is assumed. At the end of the ramp the space-charge impedance is $Z^{\parallel}/n = 100\,\Omega$ for the $U^{28+}$ beam, and $|Z^{\parallel}/n| = 1\,\Omega$ for the proton beam. Depending on the chosen proton cycle (transition or no transition), the space-charge impedance is negative or positive at the ramp end.

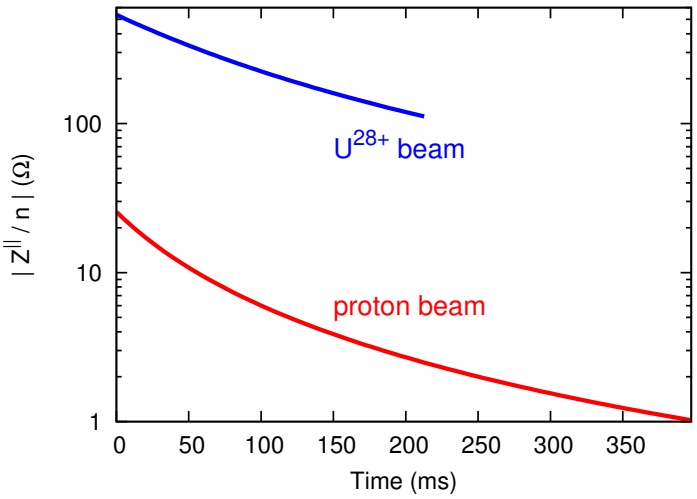


Figure 7: The longitudinal space-charge impedance for the proton beam and for the uranium beam in SIS100 along the acceleration ramp. Note the log vertical axis.

## 2.2 Resistive Wall Impedance

Similarly to the transverse resistive wall impedance, there are two types of the longitudinal impedance,

$$\text{thick}-\text{wall} \quad \delta_{\text{sk}} < d_{\text{pipe}} \ , \omega > \omega_{\text{sk}} \ , \qquad \text{Re}\Big(Z^{\parallel}_{\text{rw}}\Big) = L\frac{Z_0}{4\pi bc}\ \delta_0\sqrt{\omega_0\omega} \ , \tag{16}$$

$$\text{thin}-\text{wall} \quad \delta_{\text{sk}} > d_{\text{pipe}} \ , \omega < \omega_{\text{sk}} \ , \qquad \text{Re}\Big(Z^{\parallel}_{\text{rw}}\Big) = L\frac{Z_0}{4\pi bc}\frac{\delta_0^2\omega_0}{d_{\text{pipe}}} \ , \tag{17}$$

for a circular pipe with the radius $b$. Note that for the both cases applies

$$Z^{\perp}_{\text{rw}}(\omega) = \frac{2c}{b^2\omega}Z^{\parallel}_{\text{rw}}(\omega) \ , \tag{18}$$

compare to Eqs. (1, 2). The thin-wall $Z^{\parallel}_{\text{rw}}$ is a constant. A conservative estimation for the SIS100 resistive wall impedance can be obtained for $b = 30\,\text{mm}$, $d_{\text{pipe}} = 0.3\,\text{mm}$ and is shown Fig. 8 for $\beta = 1$. The impedance values at the bunch spectrum cutoffs are:

| Bunch Length $t_b = 4\sigma_t$ | Spectrum $f = 1/2\pi\sigma_t$ | $\text{Re}(Z^{\parallel}_{\text{rw}}/n)$ |
|---|---|---|
| 340 ns | 1.8 MHz | 2.1 Ω |
| 50 ns | 12.7 MHz | 0.7 Ω |

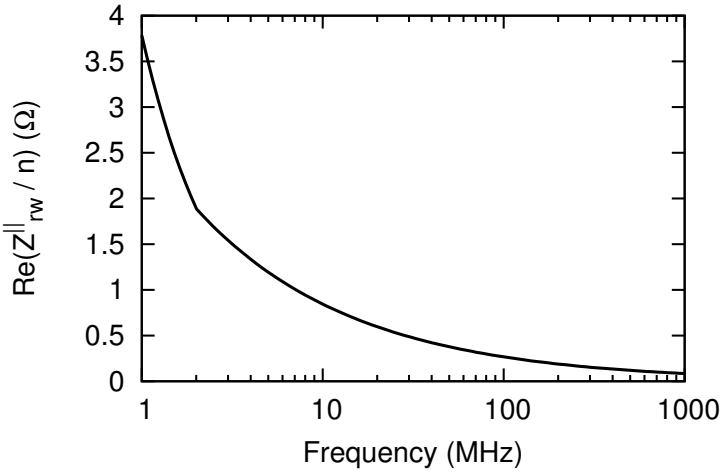


Figure 8: The SIS100 resistive wall impedance. Note that this impedance scales with relativistic $\beta$.

The imaginary impedance values are the same.

The characteristic frequency $\omega_{\parallel \mathrm{bp}}$ below which the longitudinal impedance falls to zero can be obtained using involved calculations. For a pipe with $b = 40\,\mathrm{mm}$, $d_{\mathrm{pipe}} = 0.3\,\mathrm{mm}$ it corresponds to $f_{\parallel \mathrm{bp}} \approx 3\,\mathrm{kHz}$ [4].

## 2.3 Broad-Band Longitudinal Impedance

The broad-band resonator model is usually used to approximate the complete impedance of the numerous elements of the facility,

$$Z^{\parallel}_{\mathrm{bb}} = \frac{R_{\parallel}}{1 + iQ_{\mathrm{bb}}\left(\frac{\omega}{\omega_r} - \frac{\omega_r}{\omega}\right)} \,, \tag{19}$$

with the shunt impedance $R_{\parallel}$, the quality factor $Q_{\mathrm{bb}} = 1$, and the resonant frequency $\omega_r$. The machine shunt impedance has been measured at the CERN PS synchrotron [6] $R_{\parallel} \approx 10^5\,\Omega$, with $f_r = 2.54\,\mathrm{GHz}$.

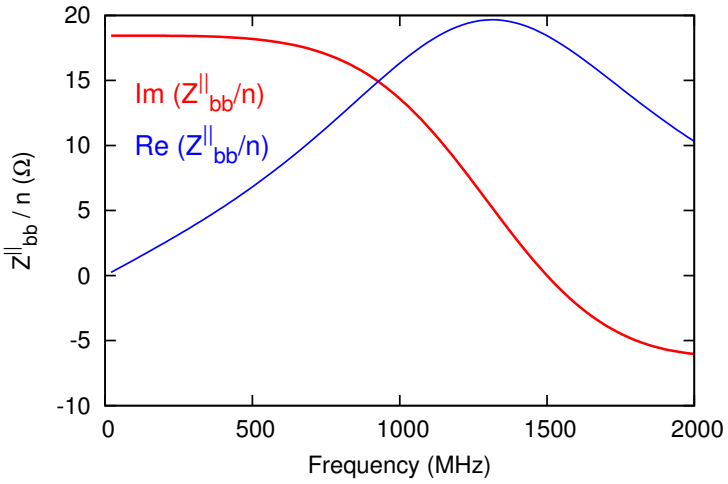


Figure 9: The SIS100 longitudinal broad-band impedance model. Note that this impedance scales with relativistic $\beta$.

For SIS100, the same shunt impedance with a different resonant frequency can be assumed,

$$R_{\parallel} \approx 10^5\,\Omega \,, \quad f_r = 1.5\,\mathrm{GHz}. \tag{20}$$

The main contributions should be given by the ferrite loaded kickers, the rf cavities, bellows and steps. This impedance is shown in Fig. 9, for $\beta = 1$. The impedance values at the bunch spectrum cutoffs are:

| Bunch Length $t_b = 4\sigma_t$ | Spectrum $f = 1/2\pi\sigma_t$ | $Z^{\parallel}_{\mathrm{bb}}/n$ |
|---|---|---|
| 340 ns | 1.8 MHz | $(0.02 + i18)\,\Omega$ |
| 50 ns | 12.7 MHz | $(0.16 + i18)\,\Omega$ |

### 2.4 Summary for the Longitudinal Impedance

The real longitudinal impedance is dominated by the resistive wall at the low frequencies of the bunch cutoffs in SIS100, see Fig. 8. Also for the shortest bunches (50 ns) the resistive wall impedance gives the main real contribution. At the higher frequencies (above 0.1 GHz) the broad-band impedance should become important for the real longitudinal impedance.

The imaginary impedance is dominated by space charge and by the broad-band composition. The space charge impedance is strong at the low energies. For the injection energies, it is $Z^{\parallel}/n = i540\,\Omega$ for the uranium beam and $Z^{\parallel}/n = i26\,\Omega$ for the proton beam. In the case of the proton beams at higher energies, the imaginary longitudinal impedance is dominated by the broad-band impedance, $Z^{\parallel}/n \approx i18\,\Omega$ for the relevant frequencies below 1 GHz.

## References


[1] FAIR - Baseline Technical Report, September 2006: http://www.gsi.de/fair/reports/btr.html

[2] L. Vos, CERN-AB-2003-005 (2003)

[3] A.M. Al-khateeb, O. Boine-Frankenheim, R.W. Hasse, and I. Hofmann, Phys. Rev. E **71**, 026501 (2005)

[4] U. Niedermayer, O. Boine-Frankenheim, Nucl. Instrum. Methods Phys. Res. A **687** 51-61 (2012)

[5] R.L. Gluckstern, Analytic methods for calculating coupling impedances, CERN 2000-011 (2000)

[6] H. Damerau, et. al., CERN-ATS-Note-2012-064 MD (2012)

[7] R.Cappi, et. al., Proc. EPAC2000, Vienna, Austria, p. 1152 (2000)

[8] K.Y. Ng, Physics of Intensity Dependent Beam Instabilities, World Scientific (2006)

[9] G. Nassibian, F. Sacherer, Nucl. Instrum. Methods **159** 21-27 (1979)